Aging Cell (2012) **11,** pp41–50 Doi: 10.1111/j.1474-9726.2011.00754.x

Increased dosage of tumor suppressors limits the tumorigenicity of iPS cells without affecting their pluripotency

Sergio Menendez,[1] Suzanne Camus,[1,*] Aida Herreria,[1,*] Ida Paramonov,[1] Laura B. Morera,[1] Manuel Collado,[2] Vlad Pekarik,[1] Iago Maceda,[1] Michael Edel,[1,3,†] Antonella Consiglio,[1,4,‡] Adriana Sanchez,[1,‡] Han Li,[2] Manuel Serrano[2] and Juan C. I. Belmonte[1,5]

[1]Center for Regenerative Medicine in Barcelona, C/Dr. Aiguarder 88, Barcelona 08003, Spain
[2]Tumor Suppression Group, Spanish National Cancer Research Centre (CNIO), 3 Melchor Fernandez Almagro Street, Madrid E-28029, Spain
[3]Honorary Research Fellow, Molecular Cardiology and Biophysics, Victor Chang Cardiac Research Institute, Sydney, NSW 2010, Australia
[4]Department of Biomedical Science and Biotechnology, University of Brescia, Viale Europa 11, 25123 Brescia, Italy
[5]Gene Expression Laboratory, Salk Institute for Biological Studies, 10010 North Torrey Pines Road, La Jolla, CA 92037, USA

Summary

Embryonic stem (ES) cells and induced pluripotent stem (iPS) cells represent a promising therapeutic tool for many diseases, including aged tissues and organs at high risk of failure. However, the intrinsic self-renewal and pluripotency of ES and iPS cells make them tumorigenic, and hence, the risk of tumor development hinders their clinical application. Here, we present a novel approach to limit their tumorigenicity and increase their safety through increased copy number of tumor suppressors. iPS containing an extra copy of the *p53* or *Ink4a/ARF* locus show normal pluripotency, as determined by *in vitro* and *in vivo* differentiation assays. Yet, while retaining full pluripotency, they also possess an improved engagement of the p53 pathway during teratocarcinoma formation, which leads to a reduced tumorigenic potential in various *in vitro* and *in vivo* assays. Furthermore, they show an improved response to anticancer drugs, which could aid in their elimination in case tumors arise with no adverse effects on cell function or aging. Our system provides a model for studying tumor suppressor pathways during reprogramming, differentiation, and cell therapy applications. This offers an improved understanding of the pathways involved in tumor growth from engrafted pluripotent stem cells, which could facilitate the use of ES and iPS cells in regenerative medicine.

Key words: induced pluripotent stem; embryonic stem; tumorigenicity; p53; Ink4a/ARF; reprogramming.

Correspondence
Juan Carlos Izpisua Belmonte, Center for Regenerative Medicine in Barcelona, Barcelona, Spain 08003. Tel.: +34 93 316 03 00; fax: +34 93 316 03 01; e-mail izpisua@cmrb.eu

*These two authors contributed equally to this work.
†Present address: Research Institute of Hospital Val d Hebron and Banc de Sang i Teixits, Advanced Cell Therapies and Immunology, 08035 Barcelona, Spain.
‡The Institute of Biomedicine of the University of Barcelona (IBUB) C. Baldiri Reixac, 15-21, 08028 Barcelona, Spain.

Accepted for publication *27 September 2011*

Introduction

The *p53* tumor suppressor gene integrates the response of multiple stress-activated pathways and plays a critical role in tumor prevention. It is estimated that p53 is directly mutated or indirectly inactivated in the majority of human tumors (Lane & Levine, 2010). Linked to the p53 pathway, the *Ink4/ARF* tumor suppressor locus encodes three important tumor suppressors, p16Ink4a and p19ARF from Cdkn2a and p15Ink4b from Cdkn2b. This locus therefore integrates two main antitumoral pathways, the p53 pathway, via the interaction of p19ARF with the p53 inhibitor protein Mdm2, and the pRB pathway, via the inhibition of cyclin-D-dependent kinases CDK4 and CDK6 by p15Ink4b and p16Ink4a (Collado & Serrano, 2006). The effect of activating these pathways in tumor prevention/treatment strategies has therefore been long studied.

However, little is known regarding the role of these tumor suppressors in tumors arising from cell therapy techniques involving embryonic stem (ES) and induced pluripotent stem (iPS) cells. Such techniques hold the promise of revolutionizing the field of regenerative medicine (Thomson *et al.*, 1998; Takahashi *et al.*, 2007), but the tumorigenic risk of iPS and ES cell replacement therapies hinders their clinical application (Blum & Benvenisty, 2008; Belmonte *et al.*, 2009; Kiuru *et al.*, 2009). Pluripotent stem cells generate benign teratomas or more aggressive teratocarcinomas upon engraftment *in vivo* (Ben-David & Benvenisty, 2011), with as few as 20 undifferentiated cells being able to generate a tumor (Lawrenz *et al.*, 2004). In addition, other sources of pluripotent or multipotent cells such as mesenchymal stem cells (MSC) or cord blood stem cells can also drive tumor formation upon engraftment *in vivo* in human patients after cell therapy (Ando *et al.*, 2006; Greaves, 2006). We hypothesized that the p53 pathway may be engaged during teratoma formation and that taking advantage of the endogenous pathways that prevent tumorigenesis could provide an attractive approach to limit the tumorigenicity of pluripotent stem cells.

However, p53 is linked to many cell processes, including metabolism and aging. The constitutive activation of p53, in fact, has been linked to a premature aging phenotype (Tyner *et al.*, 2002). As stress-induced activation of p53 leads to cell senescence, it is logical that prolonged activation of p53 would affect organismal aging. We have recently described iPS cell models that offer a relevant system to study both physiological and pathological aging (Liu *et al.*, 2011), highlighting the utility of iPS systems to model these processes.

Here, we present an iPS model system in which we employ increased dosage of the tumor suppressors *p53* and the *InK4a* locus to investigate the pathways involved in teratoma formation from ES and iPS cells used in cell therapy applications. Our models could prove useful for studying the involvement of these tumor suppressor pathways in organismal aging and aging-related pathologies. We demonstrate that increased dosage of these tumor suppressors leads to a reduced tumorigenic potential and an increased therapeutic index, in the event of tumors arising, without any apparent adverse effects on normal cell function or aging.

© 2011 The Authors
Aging Cell © 2011 Blackwell Publishing Ltd/Anatomical Society of Great Britain and Ireland

Aging Cell

Results

iPS derivation and characterization

We employed iPS cells derived from mouse embryonic fibroblasts (MEFs) harboring an extra copy of either the *p53* tumor suppressor gene (p53 super mice) (Garcia-Cao *et al.*, 2002) or the *Ink4a/ARF* tumor suppressor locus (Ink4a/ARF super mice) (Matheu *et al.*, 2004) to investigate the effect of increased tumor suppressor dose on the tumorigenic potential of pluripotent cells. Initially, we reprogrammed passage-one MEFs derived from p53 super mice (p53 iPS), Ink4a/ARF super mice (Ink4a/ARF iPS), or the parental wild-type control (wt iPS). Three individual iPS clones from each cell type were selected by morphological criteria and characterized by immunostaining for the pluripotency markers Oct4, Sox2, Nanog, and SSEA1 (Figs 1a and S1). Quantitative PCR analysis confirmed that total levels of c-Myc, Klf4, Oct4, and Nanog mRNA were comparable to the control ES cell line (Fig. S2), indicating pluripotency and silencing of the transgenes in the lines tested. All iPS lines could differentiate to the three germ layers *in vitro* (Fig. S3) and *in vivo* (Figs 1b and S4) and had normal karyotypes (Fig. S5). Furthermore, p53 and Ink4a/ARF iPS cells could contribute to chimera formation when injected into mouse blastocysts, with a success rate at least as high as that of the wt iPS cell controls in every attempt (five representative chimeric pups per condition are shown in Fig. 1c). Finally, wt, p53, and Ink4a/ARF iPS can all support germ-line transmission (Fig. 1d). These results confirm the *bona fide* pluripotent nature of the iPS generated from MEFs harboring an extra copy of p53 or Ink4a/ARF. In addition, the cell cycle profile and growth rate (Fig. 1e,f) of wt, p53, or Ink4a/ARF iPS cell lines are equivalent under normal growth conditions, indicating that the tumor suppressors are not constitutively active in the absence of stress signaling and that the presence of the extra copy of the *p53* or *Ink4a/ARF* locus has little influence on the iPS cells behavior under nonstressed conditions. These data are as expected from mouse models as the tumor suppressors are subject to the normal regulatory controls and do not show increased levels or activity under nonstressed conditions (Garcia-Cao *et al.*, 2002; Matheu *et al.*, 2004).

We further analyzed our wt, p53, and Ink4a/ARF iPS cell lines and compared them with three ES cell lines of the same genetic background using an expression profile array. As expected, all iPS cell lines have highly similar expression profiles with each other and with ES cells (Pearson correlation coefficient higher than 0.99 for all comparisons, see Figs 2a,b and S6), further confirming their *bona fide* pluripotent nature. From this analysis, we also observed that the differences in the expression profiles between wt, p53, and Ink4a/ARF iPS cell lines were comparable with the differences observed between different clones of iPS cells of the same type (shown for three different clones of wt iPS cells and one clone of wt, p53, and Ink4a/ARF iPS cells, see Fig. 2c). This indicates that under normal growth conditions the presence of one extra tumor suppressor copy has little impact on the iPS cells expression profile. These data also show that the presence of an extra copy of the *p53* or *Ink4a/ARF* locus prior

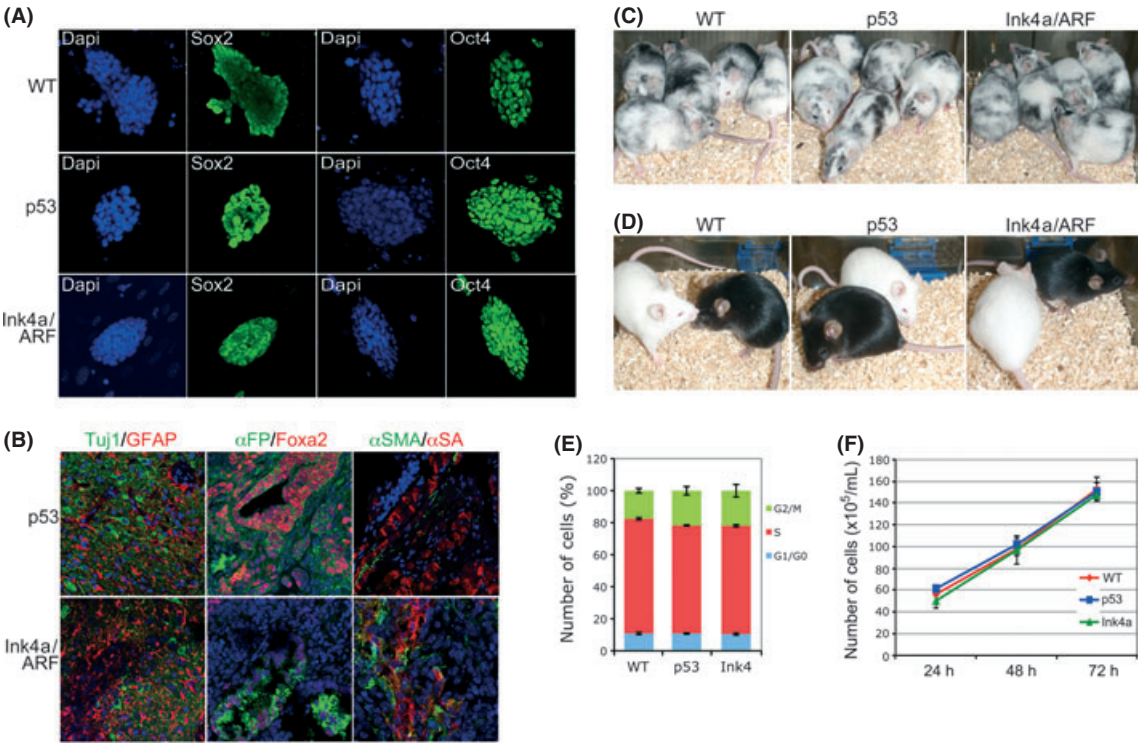

Fig. 1 wt, p53, and Ink4a/ARF induced pluripotent stem (iPS) cells show equivalent pluripotency and chimera contribution efficiency (a) wt, p53, or Ink4a/ARF iPS cell colonies grown over a mouse embryonic fibroblast (MEFs) feeder layer were stained with antibodies (Ab) against Sox2 or Oct4 as indicated. (b) wt (not shown), p53, and Ink4a iPS cells were injected intramuscularly in NOD-SCID mice (1×10^6 cells per injection). Resulting teratomas were removed when they reached an appropriate size and then fixed and analyzed by immunohistochemistry with Ab against Tuj1 (green) and GFAP (red), αFP (green) and FOXA2 (red), αSMA (green) and αSA (red) as indicated to demonstrate differentiation to the relevant germ layers. (c) wt, p53, and Ink4a/ARF iPS cells (C57BL/6J background, black coat color) were injected into 3.5-dpc blastocyst of B6(cg)-Tyrc-2J/J mice (abbreviated Tyr, white coat color) and then transferred into pseudo-pregnant Tyr recipients for chimera generation. Five representative chimeras derived from wt, p53, or Ink4a/ARF iPS cells are shown. (d) Transgenic mice derived from wt, p53, or Ink4a/ARF iPS cells are shown together with a Tyr wt control mouse. (e) FACs analysis of the cell cycle profile or (f) growth curve quantification of undifferentiated wt, p53, and Ink4a/ARF iPS cells grown in culture under nonstressed conditions show that there is no significant difference in their proliferation rate.

© 2011 The Authors
Aging Cell © 2011 Blackwell Publishing Ltd/Anatomical Society of Great Britain and Ireland

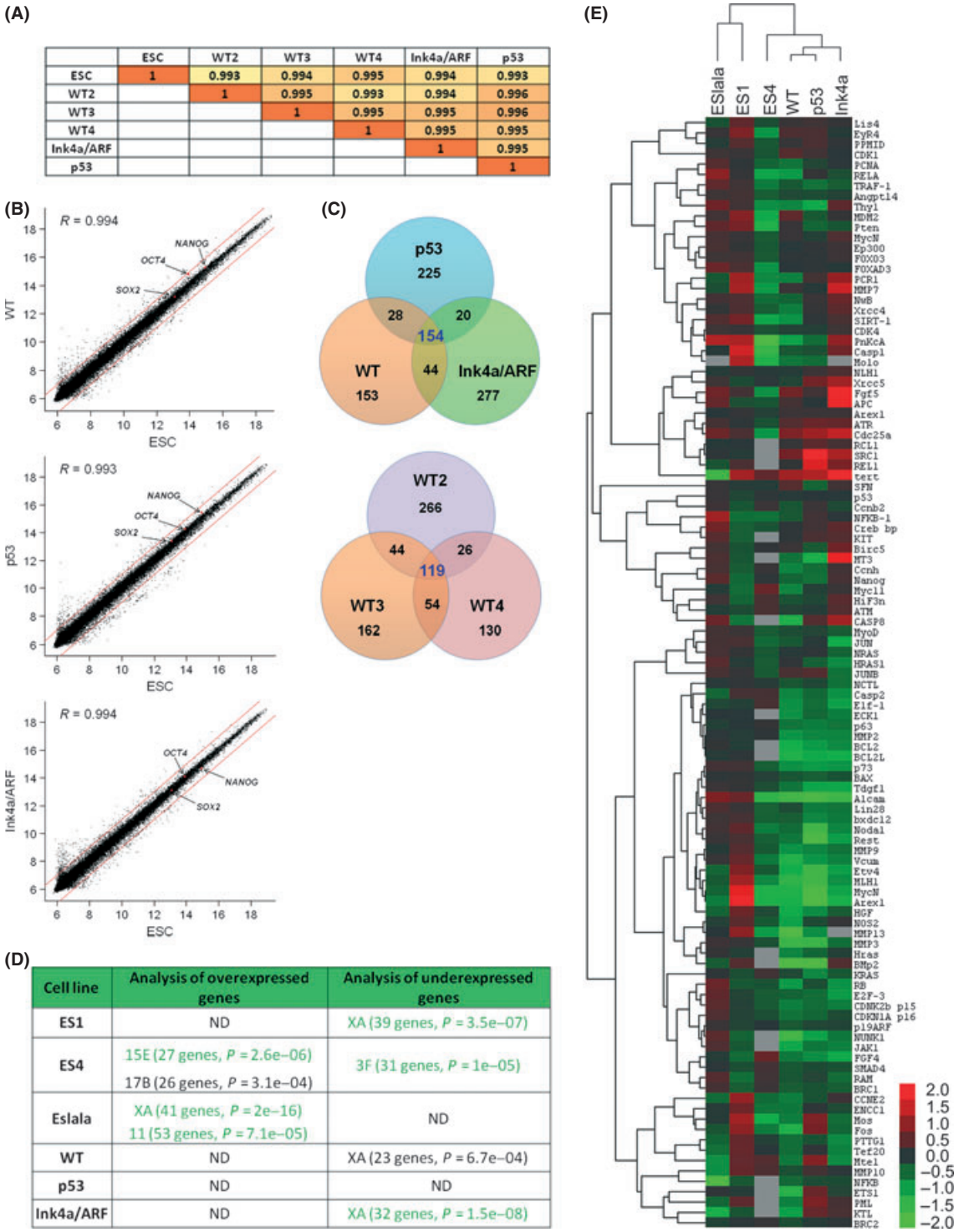

	ESC	WT2	WT3	WT4	Ink4a/ARF	p53
ESC	1	0.993	0.994	0.995	0.994	0.993
WT2		1	0.995	0.993	0.994	0.996
WT3			1	0.995	0.995	0.996
WT4				1	0.995	0.995
Ink4a/ARF					1	0.995
p53						1

(D)

Cell line	Analysis of overexpressed genes	Analysis of underexpressed genes
ES1	ND	XA (39 genes, $P = 3.5e{-}07$)
ES4	15E (27 genes, $P = 2.6e{-}06$) 17B (26 genes, $P = 3.1e{-}04$)	3F (31 genes, $P = 1e{-}05$)
Eslala	XA (41 genes, $P = 2e{-}16$) 11 (53 genes, $P = 7.1e{-}05$)	ND
WT	ND	XA (23 genes, $P = 6.7e{-}04$)
p53	ND	ND
Ink4a/ARF	ND	XA (32 genes, $P = 1.5e{-}08$)

Fig. 2 Mutation rate is not affected by increased tumor suppressor dosage. (a) Pearson correlation coefficients of the averaged expression profiles of three independent embryonic stem (ES) clones, three independent p53 induced pluripotent stem (iPS) clones, two independent Ink4a/ARF iPS clones, and three independent wt iPS clones (shown individually to highlight clonal variation among equivalent samples) are shown. (b) Scatter plots of global gene expression profiles of the average of ES versus the average of wt, p53, and Ink4a/ARF iPS cells are shown. (c) Venn diagrams showing the number of differentially expressed genes between the average of ES and the average of wt, p53, and Ink4a/ARF iPS cells (left) or three independent wt iPS cells (right) are shown. (d) Chromosomal location enrichment analysis of three independent ES cells clones and one clone of wt, p53, and Ink4a/ARF iPS cells that was used in all experiments performed throughout the manuscript unless otherwise stated is shown. *P*-values <0.0001 are highlighted in green. (e) Hierarchical clustering of ES and iPS samples described in (d) based on real-time RT-PCR data. Scale bar shows log2-transformed ratio values.

© 2011 The Authors
Aging Cell © 2011 Blackwell Publishing Ltd/Anatomical Society of Great Britain and Ireland

and during the process of reprogramming has no effect on the final expression profile of iPS cells.

Mutation rate is not affected by increased tumor suppressor dosage

Mutations accumulate during the reprogramming process in at least a proportion of iPS cell lines (Mayshar *et al.*, 2010; Gore *et al.*, 2011; Hussein *et al.*, 2011). Because p53 protects proliferating cells from the accumulation of mutations, it is possible that an increased copy number could limit the accumulation of mutations during reprogramming. Our direct analysis of the expression profile array data suggests that this is not the case in the clones that we have analyzed (three wt-, three p53-, and two Ink4a/ARF-independent iPS cell clones). However, to further explore this possibility, we mined our expression profile array data to look for large duplications or deletions accumulated during reprogramming. A similar approach has already been validated and has a sensitivity range capable of identifying duplications or deletions from 10 kb in size (Mayshar *et al.*, 2010). We did not identify any highly significant overrepresentation of overexpressed or underexpressed genes in our wt, p53, or Ink4a/ARF iPS cell lines or in our control ES cell lines (Fig. 2d), indicating that there were no detectable large duplications or deletions in our iPS or ES lines. The differences observed between our wt, p53, or Ink4a/ARF iPS cell lines were at the level that could be expected from clonal variation, as quantitatively similar variations were observed among the three ES lines used as a control (Fig. 2d). As the mutational changes reported to accumulate during reprogramming are biased toward loss of tumor suppressor and/or gain of oncogenes (Gore *et al.*, 2011; Hussein *et al.*, 2011), to further validate our conclusions, we designed a 'focused array' based on tumor suppressors, oncogenes, and genes involved in various aspects of cancer such as metastasis, intercellular interactions, and transduction signaling. We then performed quantitative real-time PCR analysis to measure mRNA expression for this gene set in our wt, p53, or Ink4a/ARF iPS cell lines using three clones of ES cells as a baseline (Figs 2e and S7). In agreement with our mRNA array data, we did not observe any differences in mRNA expression between our wt, p53, or Ink4a/ARF iPS cell lines beyond the clonal variation seen among our reference ES cell lines, further confirming that the presence of the tumor suppressor transgenes during reprogramming did not alter the iPS cell lines obtained.

Increased p53 or Ink4a/ARF dosage reduces the tumorigenic potential of iPS cells

We then tested the effect of increased p53 or Ink4a/ARF copy number on the tumorigenic potential of iPS cells. Firstly, we performed soft agar growth assays, which are a standard test of tumorigenicity that reflects the capacity of a cell to grow in conditions of low nutrients and low oxygen and in an anchorage-independent manner. A marked reduction in the growth of p53 and Ink4a/ARF iPS cells was observed compared with the wt control for several independent iPS clones, indicating that the tumorigenic potential of p53 and Ink4a iPS is reduced compared with wt cells and that this is independent of differences caused by retroviral insertion (Fig. 3a). To study the tumorigenic potential of engrafted iPS cells *in vivo*, we performed long-term and short-term teratoma assays (see Data S1). These assays are not a measurement of the pluripotency of the iPS cells (which has already been demonstrated in Figs 1 and S1–S4) as the cells were injected under 'nonsaturating' conditions (as detailed in Data S1) and are therefore informative in relation to the comparative efficiency with which the different cell lines can give rise to tumors. In long-term teratoma formation assays, in which animals were sacrificed depending on stringent predefined health parameters (see Experimental procedures), a substantial reduction in teratoma formation in mice injected with p53 and Ink4a/ARF iPS was observed compared with wt iPS (Fig. 3b,c). Interestingly, some Ink4a/ARF iPS-injected mice failed to develop any teratomas for the entire duration of the assay (Figs 3b and S8). In agreement, in short-term teratoma assays, in which the end point was predetermined, a decrease in tumor size and weight was observed for p53 iPS- and Ink4a/ARF iPS- compared with wt iPS-injected mice. Again, p53 iPS- and Ink4a/ARF iPS-injected individuals were observed that failed to develop teratomas throughout the duration of the assay, whereas teratomas were formed in all wt-injected animals (Figs 3d,e and S9). Importantly, we observed a clear decrease in the proliferation rate of p53 iPS- and Ink4a/ARF iPS-derived teratomas compared with the wt control (Fig. 3e). This is in stark contrast to undifferentiated iPS in non-stressed culture conditions, where there was no difference in the proliferation rate between wt, p53, and Ink4a/ARF cells (Fig. 1e,f). We did not observe an increase in the apoptotic rate in these tumors (data not shown), suggesting that limited proliferation was a major cause for the reduction in tumor size and number in p53 iPS- and Ink4a/ARF iPS-derived teratomas. Tumors derived from injection of mouse iPS in immunocompromised mice have been shown to contain a malignant undifferentiated population of embryonic carcinoma (EC) cells and, therefore, should be categorized as teratocarcinomas (Blum *et al.*, 2009). This EC cell component is positive for the EC markers Oct4 and Nanog and is responsible for the proliferation of the tumor and its capability to form secondary teratomas (Blum & Benvenisty, 2008). When the EC compartment of our teratomas was analyzed, we observed a marked decrease in the percentage of Oct4-positive cells in the p53- and Ink4a/ARF-derived teratocarcinomas (Figs 3f and S10). By dissociation of the teratocarcinomas, we isolated EC cells that could be passaged *in vitro*. As expected, we obtained a higher proportion of EC cells from wt iPS-derived teratocarcinomas than from p53 iPS- or Ink4a/ARF iPS-derived teratocarcinomas (Fig. 3g). Together, these results demonstrate that p53 and Ink4a/ARF iPS have decreased tumorigenicity compared with wt iPS in a range of established *in vitro* and *in vivo* assays.

Increased tumor suppressor dosage reduces the tumorigenic potential of differentiated iPS cells

We next studied the tumorigenic potential of the p53 and Ink4a/ARF iPS in an *in vivo* context relevant for cell therapy. In this regard, we differentiated iPS lines into skeletal muscle (Mizuno *et al.*, 2010) (Fig. 4a,b), a therapeutically relevant cell type that can be used in the treatment for muscular dystrophies (Darabi *et al.*, 2008), and injected them into the skeletal muscle tissue of NOD-SCID mice. We injected a nonpurified population of differentiated cells for all three cells types. These populations did not contain Oct4- or Nanog-positive cells at the detection level achieved by FACs analysis (data not shown); however, a small amount of *Nanog* and *Oct4* mRNA was still detectable in the samples by quantitative real-time PCR (data not shown), indicating that some undifferentiated cells still remained in the injected sample. Teratocarcinomas arose in all of the wt iPS cell-injected mice; however fewer and, when present, smaller tumors were observed in both the p53 iPS- and Ink4a/ARF iPS-injected littermates, indicating that the increased dosage of *p53* or *Ink4a/ARF* offers substantial protection against teratocarcinoma formation in this system (Fig. 4c). Importantly, we detected a differential induction of the p53, p21Cip1, p19ARF, and p16INK4a proteins in teratocarcinomas derived from p53 and INK4a/ARF iPS cells compared with wt iPS-derived teratocarcinomas (Figs 4d and S11). This demonstrates a more effective

© 2011 The Authors
Aging Cell © 2011 Blackwell Publishing Ltd/Anatomical Society of Great Britain and Ireland

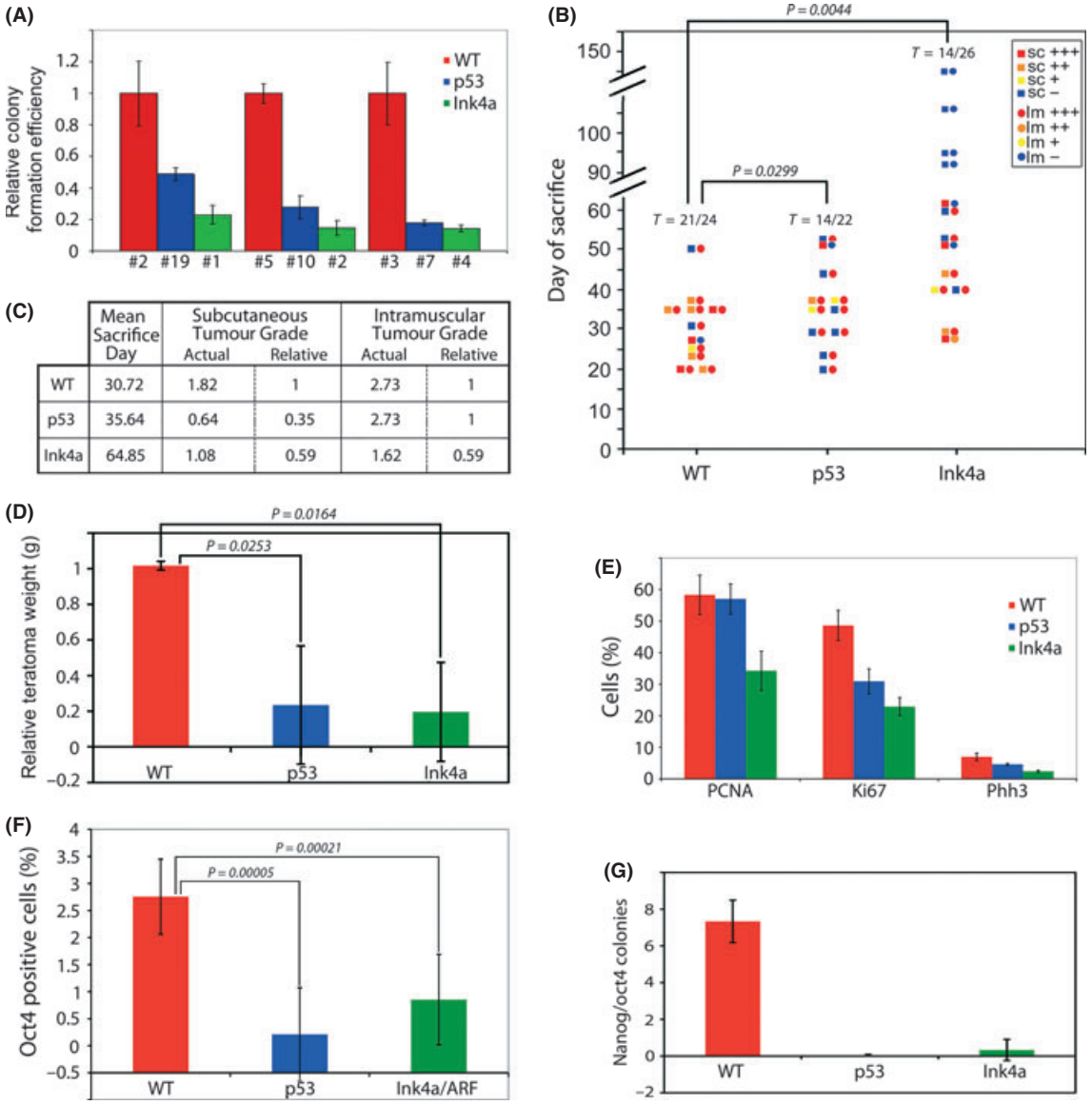

	Mean Sacrifice Day	Subcutaneous Tumour Grade		Intramuscular Tumour Grade	
		Actual	Relative	Actual	Relative
WT	30.72	1.82	1	2.73	1
p53	35.64	0.64	0.35	2.73	1
Ink4a	64.85	1.08	0.59	1.62	0.59

Fig. 3 Increased p53 or Ink4a/ARF dosage reduces the tumorigenic potential of induced pluripotent stem (iPS) cells. (a) Soft agar colony formation assays were performed with three different clones of wt, p53, or Ink4a/ARF iPS cells. Cells were grown for approximately 2 weeks, fixed, and stained, and the total number of colonies was quantified. The colony formation efficiency corresponding to each clone was calculated by dividing the total number of colonies by the initial number of cells seeded. The relative colony formation efficiency of the different clones was then calculated against that of the wt iPS cells and plotted as shown. (b) Long-term teratoma formation assay. wt, p53, or Ink4a/ARF iPS cells were injected intramuscularly and subcutaneously (1×10^5 cells per injection point, and one intramuscular and one subcutaneous injection point per animal) in NOD-SCID mice. Animals were sacrificed after tumor formation following stringent predetermined parameters (see Data S1) at a time advised by a specialized veterinarian. Teratomas formed were measured and fixed for further analysis at the point of sacrifice. The day of sacrifice, teratoma presence (□ = subcutaneous, ○ = intramuscular), and grade (+++ 2 cm teratoma, ++ 1–2 cm teratoma, + teratoma smaller than 1 cm, and – no teratoma) are plotted. T = the number of teratomas formed out of the total number injected. A Student t-test statistical analysis was performed on the total teratoma number for p53 or Ink4a/ARF iPS versus the wt iPS-injected animals. *P*-values are indicated. (c) Table summarizes the results from b. The mean sacrifice day and the mean actual and relative (as compared with the wt control) tumor grade for the subcutaneous and intramuscular tumors derived from injection of wt, p53, or Ink4a/ARF iPS cells are represented. Mean tumor grade was calculated assigning an arbitrary value of three to 2-cm tumors (+++), two to 1- to 2-cm tumors (++), one to tumors smaller than 1 cm (+) and zero to absence of tumor (–). (d) Short-term teratoma experiment. wt, p53, or Ink4a/ARF iPS cells were injected intramuscularly and subcutaneously (1×10^5 cells per injection point) in NOD-SCID mice. Four weeks after injection, mice were sacrificed and the resulting teratomas were extracted and weighed. The mean intramuscular teratoma weight is represented relative to the wt. Statistical analysis was performed as in b. (e) Proliferation analysis of the wt-, p53-, or Ink4a/ARF iPS-derived teratomas. After extraction, teratomas were fixed, sectioned, and stained with Ab against the proliferation markers PCNA, Ki67, and phospho-histone H3 (Phh3). Sections from the whole length of each teratoma were stained and quantified using MetaMorph software. Percentage of positive cells for each marker is represented as shown. (f) Graph shows the percentage of Oct4-positive cells present in teratomas from wt-, p53- and Ink4a/ARF iPS-injected mice, as indicated. At least three sections of two independent teratomas per condition were quantified. Statistical analysis was performed as in b. (g) wt-, p53-, or Ink4a/ARF-derived teratomas were extracted, disaggregated to a single-cell suspension. The cells were counted, then plated on slide flasks, and stained for the embryonic carcinoma cell markers Oct4 and Nanog. Double positive colonies after seeding of 1×10^5 cells were quantified and plotted for each condition.

© 2011 The Authors
Aging Cell © 2011 Blackwell Publishing Ltd/Anatomical Society of Great Britain and Ireland

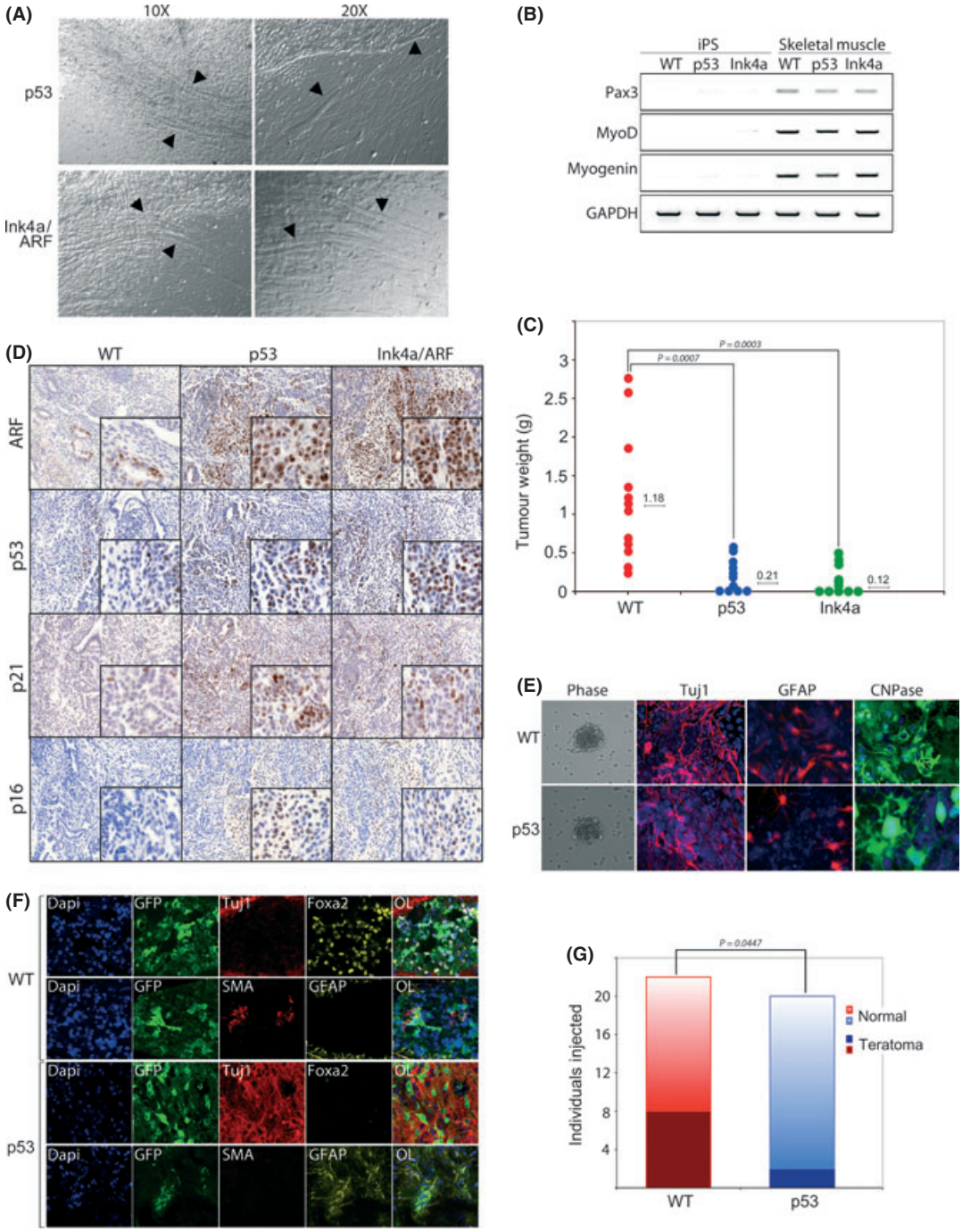

Fig. 4 Increased tumor suppressor dosage reduces the tumorigenic potential of differentiated induced pluripotent stem (iPS) cells. (a) Bright-field images of p53 and Ink4a/ARF iPS differentiated to skeletal muscle. Arrowheads identify individual muscle fibers at 10× and 20× magnification. (b) Reverse transcription PCR for the skeletal muscle markers Pax3, MyoD, and Myogenin in undifferentiated iPS and iPS differentiated to skeletal muscle. (c) Graph showing the weight of each individual teratoma and the overall mean teratoma weight from wt, p53, and Ink4a/ARF skeletal muscle differentiated cells injected intramuscularly in the gastrocnemius of NOD-SCID mice. A Student t-test statistical analysis was performed for p53 or Ink4a/ARF iPS versus the wt iPS, and *P*-values are indicated. (d) Analysis of the proportion of p19ARF-, p53-, p21Cip1, and p16Ink4-positive cells present in teratomas from wt-, p53-, and Ink4a/ARF iPS-injected mice, as indicated. At least three sections of three independent teratomas per condition were analyzed. One representative section is shown per condition. For further images, please see Fig. S10. (e) Generation of functional neurospheres (NS) from wt and p53 iPS. Bright-field image of primary NS and staining of primary NS differentiated on laminin with the neuronal marker Tuj1, the astrocyte marker GFAP, and the oligodendricyte marker CNPase as indicated. (f) Images from the engraftment area (p53) or teratomas (wt) originating from injection of disaggregated primary NS into the right striatum of NOD-SCID mice (5×10^5 cells per injection point). iPS cells were labeled with GFP using lentiviral infection prior to the differentiation in order to be able to track cell engraftment *in vivo*. A representative example of one of the teratomas generated from wt iPS positive for the endodermal marker FOXA2 and the mesodermal marker SMA is shown as indicated. A representative example of engrafted cells from p53 iPS NS positive for the neuronal lineage markers Tuj1 and GFAP and negative for endodermal or ectodermal markers is shown as indicated. (g) Quantification of the teratomas arising from wt iPS NS or p53 iPS NS under our experimental conditions. Statistical analysis was performed as in c.

© 2011 The Authors
Aging Cell © 2011 Blackwell Publishing Ltd/Anatomical Society of Great Britain and Ireland

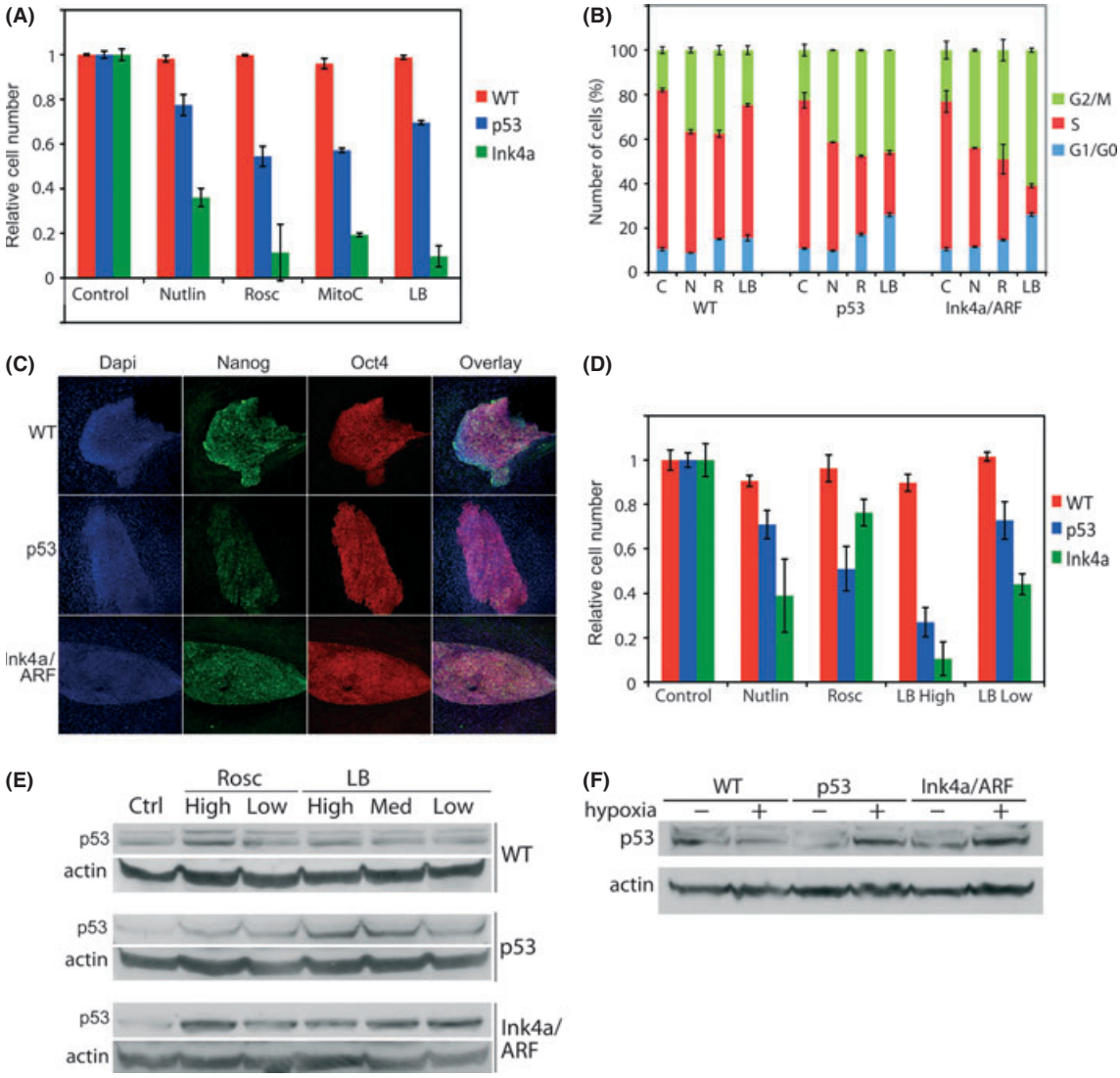

Fig. 5 Transgenic mice derived from p53 induced pluripotent stem (iPS) cells show reduced tumor formation and no aging phenotype. (a) wt, p53, and Ink4a/ARF iPS cells were treated with the antitumoral drugs nutlin-3 (2 μM final concentration), R-roscovitine (2 μM), mitomycinC (1 μg ml^{-1}), or leptomycin B (0.2 nM) for 48 h and then fixed, stained, and quantified. A quantification of the cell number in the presence of each drug relative to the untreated control is shown. (b) The cell cycle profile of wt, p53, and Ink4a/ARF iPS drugged overnight with nutlin-3 (N), roscovitine (R), and leptomycin B (LB) was analyzed by FACs. The percentage of cells in the G1, S, and G2/M phases of cell cycle for the treated and untreated control cells was quantified. (c) Cells derived from wt, p53, and Ink4a/ARF iPS teratomas were isolated and grown in culture. Embryonic carcinoma (EC) cell colonies were identified by double staining with Ab against Nanog and Oct4, as indicated. (d) EC cells were treated with the antitumoral drugs nutlin-3, roscovitine (Rosc, 2 μM), or two concentrations of leptomycin B (LB high, 0.4 nM and LB low, 0.2 nM) and quantified as in (a). (e) iPS cells were treated with the antitumoral drugs roscovitine (low, 2 μM or high, 4 μM) or leptomycin B (LB high 0.4 nM; LB medium 0.2 nM; and LB low 0.1 nM) for 24 h. p53 levels were analyzed by western blot in wt, p53, or INK4a/ARF iPS cells as indicated. Actin levels are shown as an internal control. (f) iPS cells were placed under normal growth conditions or under hypoxia (1% oxygen) and low nutrients (1% FCS) conditions for 16 h. p53 levels were analyzed by western blot in wt, p53, or INK4a/ARF iPS cells as indicated. Actin levels are shown as an internal control.

engagement of the p53 and INK4a/ARF pathways in the p53 iPS- and INK4a/ARF iPS-derived teratocarcinomas and agrees with the reduced proliferation observed in these teratocarcinomas (Fig. 4c). Furthermore, there was no significant difference in the induction of differentiation markers or reduction in pluripotency markers between wt, p53, and INK4a/ARF iPS cells upon differentiation, either in general nonlineage-directed differentiation protocols or in specific differentiation to skeletal muscle (Figs S12 and 4b). This supports a direct role of the differential activation of p53 and INK4a/ARF in limiting teratocarcinoma formation and proliferation *in vivo*.

To further study the effect of increased dosage of *p53* in an additional *in vivo* context relevant for cell therapy, we performed differentiation to primary neurospheres (NS) (Fig. 4e) and injected the disaggregated NS into the striatum of NOD-SCID mice, an assay previously used to quantify tumorigenicity in iPS cells (Miura *et al.*, 2009). In this assay, the engrafted cells are still not terminally differentiated progenitor cells. Therefore, they still retain some multipotency and can be differentiated into three different cell types: astrocytes, oligodendrocytes, and neurons. In this context, we observed a significant reduction in the formation of teratomas in p53 cells compared with wt cells with a similar engraftment level for both cell types (Fig. 4f,g), while the p53 iPS cells retain an intact capacity to differentiate into neuronal cells (as determined by positive Tuj1 staining, Fig. 4f), highlighting in an additional *in vivo* differentiation context their bona fide pluripotent nature. These results further indicate that the p53

© 2011 The Authors
Aging Cell © 2011 Blackwell Publishing Ltd/Anatomical Society of Great Britain and Ireland

pathway is engaged in a wide range of cellular contexts during teratoma formation and that the protective effect against tumor formation obtained by increasing p53 copy number is valid for a range of differentiation strategies for cell therapy.

Increased dosage of tumor suppressors offers an improved therapeutic index

Because the p53 and pRB pathways are two of the main pathways engaged during the antiproliferative response elicited by antitumoral drugs (Vazquez *et al.*, 2008; Brown *et al.*, 2009), we next investigated whether the extra copy of *p53* or *Ink4a/ARF* confers an improved therapeutic index. We therefore treated wt, p53, and Ink4a/ARF iPS cells with a panel of antitumoral drugs, including drugs currently used therapeutically or undergoing clinical trials. Using a lower concentration than normally administered, we observed a strong antiproliferative effect upon treatment of p53 and, especially, Ink4a/ARF iPS cells, whereas little or no reduction in proliferation was observed in wt iPS cells (Fig. 5a). As drugs that have no effect on DNA integrity are more suitable candidates for chemotherapy, we studied the effect of such drugs on the cell cycle profile of our iPS cell lines. As expected, these drugs have a more profound effect on the cell cycle profile of p53 and Ink4a/ARF iPS cells than on wt control cells, inducing a significant arrest in G1 and G2/M in short-term assays (Fig. 5b), which correlates with the antiproliferative effect elicited in colony formation assays (Fig. 5a). These results also demonstrate in an *in vitro* context that a differential activation of the p53 pathway occurs in iPS with increased tumor suppressor dosage under a wide range of stress signaling conditions, ranging from DNA damage to nuclear export inhibition. This is in clear contrast to the behavior of p53 and Ink4a/ARF iPS cells under nonstressed conditions, which is undistinguishable from the wt control iPS cells (see Figs 1 and 2).

Furthermore, these results were recapitulated by treatment of EC cell lines (characterized by Nanog and Oct4 double staining, Fig. 5c) derived from the teratocarcinomas generated from injection of our iPS cell lines (Fig. 5d). In agreement with this, we observed a differential induction of the p53 protein and of p53 target genes (Figs 5e and S13) upon drug treatment in p53 and INK4a/ARF iPS cells versus wt iPS cells, supporting that a more effective engagement of the p53 pathway in p53 and INK4a/ARF iPS cells is responsible for the improved therapeutic index observed in these cells. In addition, treatment with low concentrations of these antitumoral drugs could specifically target tumor cells arising from cell therapy using iPS cells that contain an extra copy of the *p53* and *Ink4a/ARF* genes. Therefore, increased p53 and Ink4a/ARF dosage could offer a substantially improved therapeutic index in this tumor type, potentially limiting side effects of the chemotherapy and allowing for a more specific targeting of the tumor cell population. Finally, we observed a differential induction of the p53 protein upon low nutrient and hypoxia conditions in p53 and INK4a/ARF iPS cells versus wt iPS cells *in vitro* (Fig. 5f), providing evidence that low-nutrient and hypoxia-mediated stress pathways could drive the differential activation of the p53 and INK4a pathways, decreased growth rate and decreased EC cell compartment observed in p53 iPS- and INK4a/ARF iPS-derived teratocarcinomas compared with wt iPS-derived teratocarcinomas in all conditions studied (Figs 3 and 4).

Transgenic mice derived from p53 iPS cells show reduced tumor formation and no aging phenotype

The tumorigenicity of iPS cells has also been studied in the context of classical tumor development in transgenic animals generated from iPS. In this context, tumor formation is triggered by reactivation of the transgenes used for reprogramming (Okita *et al.*, 2007). These studies provide interesting information regarding the stability of transgene silencing upon germ-line transmission induced modifications and have been widely used to score the tumorigenicity of iPS cells. In this line, we have generated a significant number of transgenic mice (approximately 100 mice per condition, aged between 4 and 12 months) from our p53 and wt iPS cells lines to study the effect of the increased tumor suppressor copy number on tumor development in this context. According to previous reports (Okita *et al.*, 2007; Nakagawa *et al.*, 2010), iPS-derived mice developed tumors owing to c-myc reactivation within a time frame of 2–10 months from birth. We observed tumors arising in wt iPS-derived mice with a 5% incidence owing to c-Myc reactivation, whereas no tumors have arisen in the p53 iPS-derived transgenic mice (Fig. S14 and data not shown). These results suggest that transgenic mice containing an extra copy of the p53 locus are resistant to tumor development because of c-myc reactivation. No other health changes or abnormal aging phenotypes were observed in our p53 iPS-derived transgenic mouse colony compared with their wt counterparts.

Discussion

Here, we have employed standard assays used to analyze tumorigenicity, such as soft agar assays and teratoma formation assays, as well as assays that analyze the tumorigenicity of our iPS cells in an *in vivo* context relevant for cell therapy, mimicking the conditions that are encountered in such applications, namely the engraftment of progenitors or terminally differentiated cells in a relevant tissue. Importantly, we demonstrate a significant reduction in tumorigenicity of p53 and INK4a/ARF iPS cells versus wt iPS cells in all the different conditions studied, without affecting their intrinsic properties under nonstressed growth conditions.

Interestingly, there were no adverse health effects in transgenic mice derived from p53 iPS cells and no observation of phenotypes associated with premature aging. This is in line with the lack of constitutive activation of the tumor suppressors in p53 compared with wt iPS cells, which correlates with the fact that the increased tumor suppressor dosage caused no effect on cell cycle proliferation under nonstressed conditions. These data clearly indicate that an increased dosage of tumor suppressors that are subject to endogenous regulatory mechanisms causes no adverse effects under normal cellular conditions, despite being efficiently activated upon stress signaling.

The ability of pluripotent cells to generate teratomas does not depend on genetic transformation, and thus, teratoma growth is driven by an undifferentiated cell pool that retains a high proliferative rate and some degree of pluripotency (Blum & Benvenisty, 2009). However, like other tumors, their growth is still limited by oxygen and nutrient supply. Teratomas undergo an angiogenic switch that includes differentiation of pluripotent cells within the teratoma to form vessels (Li *et al.*, 2009). However, before this vascularization is achieved areas within the teratoma are under hypoxia conditions. Given the profound effect that the increased dosage of the *p53* and *Ink4a/ARF* locus had on the capability of iPS cells to form colonies in soft agar assays, it is likely that hypoxia- and low-nutrient stress-mediated signaling activates the p53 pathway during teratoma formation to limit growth. In agreement, hypoxia directly activates the p53 pathway (Graeber *et al.*, 1996), and a clear link between p53 and metabolism in cancer cells has recently emerged (Maddocks & Vousden, 2011). We further provide preliminary evidence of p53 activation in iPS cells upon hypoxia and low nutrient supply (Fig. 5f). However, other stress signaling pathways may also be involved in the activation of p53 during teratoma formation. In this regard, it is worth noting that DNA damage also effectively triggers the activation of p53 in ES (Menendez

© 2011 The Authors
Aging Cell © 2011 Blackwell Publishing Ltd/Anatomical Society of Great Britain and Ireland

et al., 2011) and iPS cells (Fig. 5a). In agreement with this observation, increased tumor suppressor dosage facilitates the elimination of EC cells at suboptimal concentrations of genotoxic and nongenotoxic antitumoral drugs, offering an improved therapeutic index allowing specific targeting of tumor cells with fewer expected side effects (Fig. 5).

Genetic modification of ES or iPS cells is an attractive methodology to limit their tumorigenicity, as manipulation of their genome can be easily achieved (Ellis *et al.*, 2010). Therefore, increasing the dosage of tumor suppressors could potentially be a suitable approach to limit the tumorigenicity of ES or iPS cells in a clinical context. This approach presents advantages over the elimination of tumor cells that may arise post-therapy or the selection of completely pure differentiated populations of cells for use in cells therapy (Ben-David & Benvenisty, 2011). It could be of particular interest when undifferentiated progenitor cells must be used for cell therapy or for iPS generated for the treatment for diseases that require genetic correction and, therefore, genetic manipulation of the host genome prior to cell therapy, especially if these diseases carry an intrinsic risk of genomic abnormalities (Raya *et al.*, 2009). Further optimization of the tumor suppressor transgenes used in this study remains needed owing to their large size, which hinders their use for effective gene targeting into ES and iPS cells. The design and optimization of a 'minimal tumor suppressor cassette' would therefore be required before this technology could be applied in a clinical context.

Importantly, our model provides insight into the pathways involved in the formation of teratomas from pluripotent cell sources used therapeutically. It further provides validation of the usefulness of iPS as a tool for studying tumor suppressor pathways during cell reprogramming, differentiation, and cell therapy applications, which are relevant for many contexts including tumor biology, aging, stress-activated pathways, and metabolism.

Experimental procedures

Induced pluripotent stem were generated using the four original Yamanaka pMXs retroviral vectors as described elsewhere (Kawamura *et al.*, 2009). The same clones of wt, p53, and Ink4a/ARF iPS cells were used in all experiments described in the manuscript unless otherwise stated. Embryonic stem and iPS cells were used between passages 6–10. Immunostaining of iPS colonies, teratomas and quantification of staining were performed as described elsewhere (Kawamura *et al.*, 2009) and in Data S1. Teratoma formation assays were performed following standard procedures, using a lower cell number for injection (1×10^5 iPS cells per subcutaneous or intramuscular injection point unless otherwise stated). Real-time PCR, RT-PCR, FACS analysis, soft agar assays, drug treatments, cell quantification, and EC cell isolation from disaggregated teratomas were also performed according to standard procedures; differentiation to skeletal muscle (Mizuno *et al.*, 2010), primary neurospheres (Miura *et al.*, 2009), and general differentiation protocols was optimized from published protocols. For expression profile analysis, the samples were hybridized to the Agilent SurePrint G3 Mouse Gene Expression 8×60K Microarray, following standard procedures at the Center Regulation Genomica Barcelona array facility. Microarray analysis was performed following standard protocols, and detail information can be found in the Data S1. Hierarchical clustering of qRT-PCR samples was performed on log2-transformed ratio values using correlation metric and the average linkage method with Cluster software and visualized by TreeView software (Eisen *et al.*, 1998). Mouse husbandry and care followed standard procedures. Further details of all protocols can be found in the Data S1.

Acknowledgments

We are grateful to the CMRB Histology and Bioimaging, Flow Cytometry, Cell Culture, and Embryo Micromanipulation platforms. We would also like to thank Ignasi Rodríguez-Pizà for sharing expertise for teratoma formation assays and Stephanie Boue for helpful discussions. A.C was supported in part by the Programa Ramon y Cajal from the MICINN. Additional support was provided by grants from MICINN (BFU2010-21823 to A.C), and Fondazione Guido Berlucchi 2010 to A.C. Work in the laboratory of J.C.I.B was supported by grants from MICINN, Tercel, G. Harold and Leila Y. Mathers Charitable Foundation, The Leona M. and Harry B. Helmsley Charitable Trust, and Fundacion Cellex.

Author contributions

SM designed and performed experiments and wrote the manuscript. SC performed experiments and wrote the manuscript. AH performed experiments and help to design and monitor the *in vivo* experiments. IB performed bioinformatics analysis. LBM generated the chimeras and transgenic mice. IM performed quantitative PCR experiments. MJE performed soft agar assays. VP, AC, and AS helped with the neurosphere differentiation and injection protocol. HL and MC performed reprogramming and histological analysis. MS provided reagents and guidance. J.C.I.B provided direction and guidance for the various aspects of the project.

References

Ando T, Yujiri T, Mitani N, Takeuchi H, Nomiyama J, Suguchi M, Matsubara A, Tanizawa Y (2006) Donor cell-derived acute myeloid leukemia after unrelated umbilical cord blood transplantation. *Leukemia* **20**, 744–745.

Belmonte JC, Ellis J, Hochedlinger K, Yamanaka S (2009) Induced pluripotent stem cells and reprogramming: seeing the science through the hype. *Nat. Rev. Genet.* **10**, 878–883.

Ben-David U, Benvenisty N (2011) The tumorigenicity of human embryonic and induced pluripotent stem cells. *Nat. Rev. Cancer* **11**, 268–277.

Blum B, Benvenisty N (2008) The tumorigenicity of human embryonic stem cells. *Adv. Cancer Res.* **100**, 133–158.

Blum B, Benvenisty N (2009) The tumorigenicity of diploid and aneuploid human pluripotent stem cells. *Cell Cycle* **8**, 3822–3830.

Blum B, Bar-Nur O, Golan-Lev T, Benvenisty N (2009) The anti-apoptotic gene surviving contributes to teratoma formation by human embryonic stem cells. *Nat. Biotechnol.* **27**, 281–287.

Brown CJ, Lain S, Verma CS, Fersht AR, lane DP (2009) Awakening guardian angels: drugging the p53 pathway. *Nat. Rev. Cancer* **9**, 862–873.

Collado M, Serrano M (2006) The power and the promise of oncogene-induced senescence markers. *Nat. Rev. Cancer* **6**, 472–476.

Darabi R, Gehlbach K, Bachoo RM, Kamath S, Osawa M, Kamm KE, Kyba M, Perlingeiro RC (2008) Functional skeletal muscle regeneration from differentiating embryonic stem cells. *Nat. Med.* **14**, 134–143.

Eisen MB, Spellman PT, Brown PO, Botstein D (1998) Cluster analysis and display of genome-wide expression patterns. *Proc. Natl. Acad. Sci. U S A* **95**, 14863–14868.

Ellis J, Baum C, Benvenisty N, Mostoslavasky G, Okano H, Stanford WL, Porteus M, Sadelain M (2010) Benefits of utilizing gene-modified iPSCs for clinical applications. *Cell Stem Cell* **7**, 429–430.

Garcia-Cao I, Garcia-Cao M, Martin-Caballero J, Criado LM, Klatt P, Flores JM, Weill JC, Blasco MA, Serrano M (2002) ''Super p53'' mice exhibit enhanced DNA damage response, are tumor resistant and age normally. *EMBO J.* **21**, 6225–6235.

Gore A, Li Z, Fung HL, Young JE, Agarwal S, Antosiewicz-Bourget J, Canto I, Giorgetti A, Israel MA, Kiskinis E, Lee JH, Loh YH, Manos PD, Montserrat N, Panopoulos AD, Ruiz S, Wilbert ML, Yu J, Kirkness EF, Izpisua Belmonte JC,

© 2011 The Authors
Aging Cell © 2011 Blackwell Publishing Ltd/Anatomical Society of Great Britain and Ireland

Rossi DJ, Thomson JA, Eggan K, Daley GQ, Goldstein LS, Zhang K (2011) Somatic coding mutations in human induced pluripotent stem cells. *Nature* **471**, 63–67.

Graeber TG, Osmanian C, Jacks T, Housman DE, Koch CJ, Lowe SW, Giaccia AJ (1996) Hypoxia-mediated selection of cells with diminished apoptotic potential in solid tumours. *Nature* **379**, 88–91.

Greaves MF (2006) Cord blood donor cell leukemia in recipients. *Leukemia* **20**, 1633–1634.

Hussein SM, Batada NN, Vuoristo S, Ching RW, Autio R, Närvä E, Ng S, Sourour M, Hämäläinen R, Olsson C, Lundin K, Mikkola M, Trokovic R, Peitz M, Brüstle O, Bazett-Jones DP, Alitalo K, Lahesmaa R, Nagy A, Otonkoski T (2011) Copy number variation and selection during reprogramming to pluripotency. *Nature* **471**, 58–62.

Kawamura T, Suzuki J, Wang YV, Menendez S, Morera LB, Raya A, Wahl GM, Belmonte JC (2009) Linking the p53 tumour suppressor pathway to somatic cell reprogramming. *Nature* **460**, 1140–1144.

Kiuru M, Boyer JL, O'Connor TP, Crystal RG (2009) Genetic control of wayward pluripotent stem cells and their progeny after transplantation. *Cell Stem Cell* **4**, 289–300.

Lane D, Levine A (2010) P53 research: the past thirty years and the next thirty years. *Cold Spring Harb. Perspect. Biol.* **2**, a000893.

Lawrenz B, Schiller H, Willbold E, Ruediger M, Muhs A, Esser S (2004) Highly sensitive biosafety model for stem-cell-derived grafts. *Cytotherapy* **6**, 212–222.

Li Z, Huang H, Boland P, Dominguez MG, Burfeind P, Lai KM, Lin HC, Gale NW, Daly C, Auerbach W, Valenzuela D, Yancopoulos GD, Thurston G (2009) Embryonic stem cell tumor model reveals role of vascular endothelial receptor tyrosine phosphatase in regulating Tie2 pathway in tumor angiogenesis. *Proc. Natl. Acad. Sci. U S A* **106**, 22399–22404.

Liu GH, Barkho BZ, Ruiz S, Diep D, Qu J, Yang SL, Panopoulos AD, Suzuki K, Kurian L, Walsh C, Thompson J, Boue S, Fung HL, Sancho-Martinez I, Zhang K, Yates III J, Izpisua Belmonte JC (2011) Recapitulation of premature ageing with iPSCs from Hutchinson-Gilford progeria syndrome. *Nature* **472**, 221–225.

Maddocks OD, Vousden KH (2011) Metabolic regulation by p53. *J. Mol. Med.* **89**, 237–245.

Matheu A, Pantoja C, Efeyan A, Criado LM, Martín-Caballero J, Flores JM, Klatt P, Serrano M (2004) Increased gene dosage of Ink4a/Arf results in cancer resistance and normal aging. *Genes Dev.* **18**, 2736–2746.

Mayshar Y, Ben-David U, Lavon N, Biancotti JC, Yakir B, Clark AT, Plath K, Lowry WE, Benvenisty N (2010) Identification and classification of chromosomal aberrations in human induced pluripotent stem cells. *Cell Stem Cell* **7**, 521–531.

Menendez S, Goh AM, Camus S, Ng KW, Kua N, Badal V, Lane DP (2011) MDM4 downregulates p53 transcriptional activity and response to stress during differentiation. *Cell cycle* **10**, 1100–1108.

Miura K, Okada Y, Aoi T, Okada A, Takahashi K, Okita K, Nakagawa M, Koyanagi M, Tanabe K, Ohnuki M, Ogawa D, Ikeda E, Okano H, Yamanaka S (2009) Variation in the safety of induced pluripotent stem cell lines. *Nat. Biotechnol.* **27**, 743–745.

Mizuno Y, Chang H, Umeda K, Niwa A, Iwasa T, Awaya T, Fukada S, Yamamoto H, Yamanaka S, Nakahata T, Heike T (2010) Generation of skeletal muscle stem/progenitor cells from murine induced pluripotent stem cells. *FASEB J.* **24**, 2245–2253.

Nakagawa M, Takizawa N, Narita M, Ichisaka T, Yamanaka S (2010) Promotion of direct reprogramming by transformation-deficient Myc. *Proc. Natl. Acad. Sci. U S A* **107**, 14152–14157.

Okita K, Ichisaka T, Yamanaka S (2007) Generation of germline-competent induced pluripotent stem cells. *Nature* **448**, 313–317.

Raya A, Rodriguez-Piza I, Guenechea G, Vassena R, Navarro S, Barrero MJ, Consiglio A, Castellà M, Río P, Sleep E, González F, Tiscornia G, Garreta E, Aasen T, Veiga A, Verma IM, Surrallés J, Bueren J, Izpisúa Belmonte JC (2009) Disease-corrected haematopoietic progenitors from Fanconi anaemia induced pluripotent stem cells. *Nature* **460**, 53–59.

Takahashi K, Tanabe K, Ohnuki M, Narita M, Ichisaka T, Tomoda K, Yamanaka S (2007) Induction of pluripotent stem cells from adult human fibroblasts by defined factors. *Cell* **131**, 861–872.

Thomson JA, Itskovitz-Eldor J, Shapiro SS, Waknitz MA, Swiergiel JJ, Marshall VS, Jones JM (1998) Embryonic stem cell lines derived from human blastocysts. *Science* **282**, 1145–1147.

Tyner SD, Venkatachalam S, Choi J, Jones S, Ghebranious N, Igelmann H, Lu X, Soron G, Cooper B, Brayton C, Hee Park S, Thompson T, Karsenty G, Bradley A, Donehower LA (2002) p53 mutant mice that display early ageing-associated phenotypes. *Nature* **415**, 45–53.

Vazquez A, Bond EE, Levine AJ, Bond GL (2008) The genetics of the p53 pathway, apoptosis and cancer therapy. *Nat. Rev. Drug Discov.* **7**, 979–987.

Supporting Information

Additional supporting information may be found in the online version of this article:

Fig. S1 Immunostaining of iPS clones for pluripotency markers.

Fig. S2 Quantitative PCR of silenced reprogramming factors.

Fig. S3 Differentiation of iPS lines to 3 germ-layers (*in vitro*).

Fig. S4 Differentiation of iPS lines to 3 germ-layers (*in vivo*).

Fig. S5 iPS lines display normal karyotype.

Fig. S6 Hierarchical clustering of iPS and ES lines.

Fig. S7 Quantitative PCR supporting microarray data.

Fig. S8 Raw data from long-term teratoma assay.

Fig. S9 Short-term teratoma assay tumour weights and images.

Fig. S10 Oct4 staining for EC component of teratomas.

Fig. S11 antibody staining for p53, p21cip, p19ARF and p16INK4a proteins in teratocarcinomas.

Fig. S12 Quantitative PCR of differentiation and pluripotency markers following non-lineage directed differentiation of iPS lines.

Fig. S13 Differential induction of p53 target genes in iPS lines following drug treatment.

Fig. S14 Transgenic F1 mice with increased tumour suppressor dosage are protected from tumour development.

Data S1 Experimental procedures.

As a service to our authors and readers, this journal provides supporting information supplied by the authors. Such materials are peer-reviewed and may be re-organized for online delivery, but are not copy-edited or typeset. Technical support issues arising from supporting information (other than missing files) should be addressed to the authors.

© 2011 The Authors
Aging Cell © 2011 Blackwell Publishing Ltd/Anatomical Society of Great Britain and Ireland